

Electrochemically Generated Magnetic Forces. Enhanced Transport of a Paramagnetic Redox Species in Large, Nonuniform Magnetic Fields

Steven R. Ragsdale,[†] Kyle M. Grant, and Henry S. White*

Contribution from the Department of Chemistry, University of Utah, Salt Lake City, Utah 84112

Received July 20, 1998

Abstract: Electrochemically generated magnetic forces at a disk-shaped ultramicroelectrode have been investigated in large, nonuniform magnetic fields. Two sources of magnetic force are simultaneously operative in the electrochemical experiment, both having a significant influence on molecular transport of the electrochemical reactants and products. First, the magnetohydrodynamic (MHD) force, \mathbf{F}_{MHD} , described by the Lorentz equation, arises from the *diffusion of electrogenerated ions* in the magnetic field. The magnitude of \mathbf{F}_{MHD} is dependent upon the strength and orientation of the magnetic field. Second, the gradient magnetic force, \mathbf{F}_{VB} , which is proportional to the gradient of the magnetic field, arises from *electrogeneration of paramagnetic molecules* in a nonuniform magnetic field. \mathbf{F}_{VB} is dependent on the magnetic field strength, its spatial gradient, and the magnetic properties of the redox-active molecules. \mathbf{F}_{VB} and \mathbf{F}_{MHD} may be experimentally decoupled and investigated by variation of the field homogeneity and the electrode orientation. Specifically, \mathbf{F}_{MHD} is negligibly small when the surface of the ultramicroelectrode is oriented perpendicular to the magnetic field, thus allowing \mathbf{F}_{VB} to be investigated without interference from magnetohydrodynamic flows. Order-of-magnitude theoretical estimates of \mathbf{F}_{MHD} and \mathbf{F}_{VB} are correlated with voltammetric data for the electrochemical reduction of nitrobenzene at a 25- μm -radius Pt microdisk electrode in a superconducting cryomagnet. Enhancements in the voltammetric limiting current as large as $\sim 400\%$ ($B = 9.4 \text{ T}$, $\nabla B = 0 \text{ T/m}$) and $\sim 100\%$ ($B = 6 \text{ T}$, $\nabla B \sim 75 \text{ T/m}$) are associated with \mathbf{F}_{MHD} and \mathbf{F}_{VB} , respectively.

Introduction

Two sources of magnetic forces are operative whenever an electrochemical reaction is carried out in an external magnetic field. The first of these is the magnetic force acting on the charge-carrying ions, \mathbf{F}_{MHD} (N/m^3), described by the Lorentz equation, eq 1, where \mathbf{J} is the flux of ions ($\text{coulombs/cm}^2 \text{ s}$)

$$\mathbf{F}_{\text{MHD}} = \mathbf{J} \times \mathbf{B} \quad (1)$$

and \mathbf{B} is the external magnetic field (Tesla). If \mathbf{F}_{MHD} is sufficiently large, the acceleration of the charge-carrying ions results in significant momentum transfer to the solvent and counterions, setting the fluid in motion. The flow that results from \mathbf{F}_{MHD} is generally referred to as a magnetohydrodynamic (MHD) flow. MHD flows are readily observed in both uniform and nonuniform magnetic fields and are being investigated in several laboratories.^{1–19} Our laboratory has very recently demonstrated that MHD flows can be generated in nanoliter volumes of solution adjacent to the surface of a disk-shaped ultramicroelectrode (UME) and that this flow results in a significant enhancement or diminishment of the electrochemical current.^{20–23}

* To whom correspondence should be addressed. E-mail: white@chemistry.utah.edu.

[†] Current address: Broadley-James Corporation, 19 Thomas, Irvine, CA 92618.

(1) A detailed review of magnetic field effects on electrolytic processes prior to 1983 is given in: Fahidy, T. Z. *J. Appl. Electrochem.* **1983**, *13*, 553.

(2) A review describing recent progress in magnetic field effects in electrochemistry is given in: Tacke, R. A.; Janssen, L. J. *J. Appl. Electrochem.* **1995**, *25*, 1.

(3) Leventis, N.; Chen, M.; Gao, X.; Canals, M.; Zhang, P. *J. Phys. Chem.* **1998**, *102*, 3512.

The second source of the magnetic force in an electrochemical experiment has its origin in the magnetic properties of the redox molecules. For any electrochemical reaction, eq 2, the change



in the oxidation state of the molecule is accompanied by a corresponding change in magnetic susceptibility. Unless both

(4) Mogi, I.; Kido, G.; Nakagawa, Y. *Bull. Chem. Soc. Jpn.* **1990**, *63*, 1871.

(5) Mogi, I.; Kamiko, M.; Okubo, S. *Physica B* **1995**, *211*, 319.

(6) Yamamoto, I.; Yamaguchi, M.; Goto, T.; Mirura, S. *Sci. Rep.* **1996**, *A42*, 309.

(7) Yamanaka, S.; Aogaki, R.; Yamato, M.; Ito, E.; Mogi, I. *194th Rep. Inst. Mater. Res.* **1993**, 399.

(8) Takahashi, M.; Yamazaki, Y.; Inoue, A. *Int. J. Multiphase Flow* **1994**, *20*, 1095.

(9) Aogaki, R.; Negishi, T.; Yamato, M.; Ito, E.; Mogi, I. *Physica B* **1994**, *201*, 611.

(10) Mogi, I.; Watanabe, K. *Bull. Chem. Soc. Jpn.* **1997**, *70*, 2337.

(11) Inoue, Y.; Yamato, M.; Kimura, T.; Ito, E. *Synth. Met.* **1997**, *84*, 435.

(12) Mogi, I. *Chem. Lett.* **1996**, 419.

(13) Mogi, I.; Kamiko, M. *J. Cryst. Growth* **1996**, *166*, 276.

(14) Mohanta, S.; Fahidy, T. Z. *J. Appl. Electrochem.* **1978**, *8*, 265.

(15) Ismail, M. I.; Fahidy, T. Z. *Can. J. Chem. Eng.* **1979**, *57*, 734.

(16) Ismail, M. I.; Fahidy, T. Z. *Can. J. Chem. Eng.* **1980**, *58*, 505.

(17) Bobreshova, O. V.; Golitsyn, V. Y.; Timashev, S. F. *Elektrokhimiya* **1990**, *26*, 58.

(18) Mohanta, S.; Fahidy, T. Z. *Electrochim. Acta* **1976**, *21*, 149.

(19) Mogi, I.; Kamiko, M. *Sci. Rep.* **1996**, *A42*, 315.

(20) Lee, J.; Gao, X.; Hardy, L. D. A.; White, H. S. *J. Electrochem. Soc.* **1995**, *142*, L90.

(21) Ragsdale, S. R.; Lee, J.; Gao, X.; White, H. S. *J. Phys. Chem.* **1996**, *100*, 5913.

(22) Lee, J.; Ragsdale, S. R.; Gao, X.; White, H. S. *J. Electroanal. Chem.* **1997**, *422*, 169.

(23) Ragsdale, S. R.; Lee, J.; White, H. S. *Anal. Chem.* **1997**, *69*, 2070.

O and R have identical magnetic susceptibilities, the redox reaction will create a thin layer of solution near the electrode that has a volume magnetic susceptibility, χ , that is different from the corresponding value in the bulk solution. For example, consider the reduction of a neutral, diamagnetic organic molecule (with spin $S = 0$) to the corresponding radical anion ($S = 1/2$). For this reaction, χ increases significantly near the electrode surface relative to the bulk solution. In the absence of a magnetic field, the increase in spin associated with the reaction has no significant effect on electrochemical behavior. However, in the presence of an external magnetic field, a gradient force, $\mathbf{F}_{\nabla B}$ (eq 3, where μ is the magnetic permeability), will be generated in the boundary layer region.²⁴ $\mathbf{F}_{\nabla B}$ reflects the tendencies of diamagnetic and paramagnetic molecules to move away from and toward regions of higher magnetic field strength, respectively.

$$\mathbf{F}_{\nabla B} = \frac{\chi}{\mu}(\mathbf{B} \cdot \nabla) \quad (3)$$

Unlike \mathbf{F}_{MHD} , eq 3 indicates that $\mathbf{F}_{\nabla B}$ will be operative only in a nonuniform field, i.e., when $\nabla B \neq 0$.

The influence of a gradient force on electrochemical processes has only very recently been observed by O'Brien and Santhanam in their studies of a Cu/CuSO₄/Cu cell immersed in an external magnetic field.^{25,26} Paramagnetic Cu²⁺ is generated and consumed at the anode and cathode, respectively, creating a gradient in the concentration of Cu²⁺ across the cell, and thus, a corresponding gradient in the volume magnetic susceptibility. When this cell is immersed in a *uniform* external magnetic field, an internal *nonuniform* field is induced, i.e., $\nabla B \neq 0$, giving rise to a finite value of $\mathbf{F}_{\nabla B}$. This internally generated force drives fluid convection in the cell. While analogous magnetic field-controlled transport of paramagnetic liquids is of current interest in biology²⁷ and applied physics,²⁸ the report of O'Brien and Santhanam is apparently the first to suggest that this phenomenon may occur in an electrochemical cell. Tanimoto and co-workers recently reported a similar flow of paramagnetic solution during the chemical reduction of Ag⁺ on a Cu wire.^{29,30}

In this report, we demonstrate that the acceleration of electrogenerated paramagnetic molecules in a nonuniform magnetic field may result in a significant enhancement in electrochemical current. Our experiments are focused on the electrogeneration of the nitrobenzene radical anion at a 25- μm -radius Pt microdisk electrode in a large and nonuniform magnetic field. From an experimental perspective, there are two reasons why it is highly advantageous to employ a disk-shaped UME in studies of the gradient magnetic force. First, the *net* hydrodynamic force, \mathbf{F}_{MHD} , acting on the solution vanishes at a disk-shaped UME when the magnetic field is oriented orthogonal to the surface.²³ Thus, $\mathbf{F}_{\nabla B}$ can be studied with relative ease at the disk-shaped UME without interference from

(24) Equation 3 is derived by combining the expression for the magnetic force acting on unit volume, $\mathbf{F}_{\nabla B} = (\mathbf{M} \cdot \nabla)\mathbf{B}$, with the definition of the magnetic dipole per unit volume, $\mathbf{M} = (\chi/\mu)\mathbf{B}$.

(25) O'Brien, R., N.; Santhanam, K. S. V. *J. Appl. Electrochem.* **1990**, *20*, 427.

(26) O'Brien, R., N.; Santhanam, K. S. V. *J. Appl. Electrochem.* **1997**, *27*, 573.

(27) Shiga, T.; Okazaki, M.; Seiyama, A.; Maeda, N. *Bioelectrochem. Bioenerget.* **1993**, *30*, 181.

(28) Ueno, S.; Iwasaka, M. *J. Appl. Phys.* **1994**, *75*, 7177.

(29) Tanimoto, Y.; Katsuki, A.; Yano, H.; Watanabe, S. *J. Phys. Chem.* **1997**, *101*, 7359.

(30) Katsuki, A.; Watanabe, S.; Tokunga, R.; Tanimoto, Y. *Chem. Lett.* **1996**, 219.

the masking effects of \mathbf{F}_{MHD} . Second, because of the reduced ohmic potential drop, quantitative voltammetric investigations of highly concentrated redox solutions are possible with disk-shaped UME's.^{31–35} The use of highly concentrated redox solutions results in a very large spatial gradient in the volume magnetic susceptibility near the electrode surface and, thus, a large gradient in $\mathbf{F}_{\nabla B}$. Specifically, the solutions employed in the experiments reported herein contain a redox-active species at concentrations between 1 and 10 M, resulting in the *generation of molar concentrations of paramagnetic species* at the electrode surface. Thus, the disk-shaped UME appears to be an ideal electrode for fundamental investigations of $\mathbf{F}_{\nabla B}$.

The results of the current investigation demonstrate that the Faradaic current at an UME is proportional to the quantity $B\nabla B$ (eq 3, where B is the magnitude of the field, i.e., $B = |\mathbf{B}|$) in situations where $\mathbf{F}_{\nabla B}$ is anticipated to be the dominant magnetic force, *vide infra*. To our knowledge, this is the first quantitative examination of the relationship between $\mathbf{F}_{\nabla B}$ and the rate of an electrochemical reaction.

Experimental Section

Voltammetric Measurements. The Pt microdisk electrodes used throughout this study were prepared by sealing a 25- μm -radius Pt wire in a glass tube. The end of the tube was sanded flat to expose the microdisk. The disk was then polished with successively finer Al₂O₃ paste (down to ~ 0.01 – $0.02 \mu\text{m}$), rinsed and sonicated in 18 M Ω ·cm ("E-Pure") H₂O to remove polishing debris, rinsed with methanol, and air dried prior to use. The voltammetric response of the electrode was recorded in a 2 mM ferrocene/0.2 M tetra(*n*-butyl)ammonium hexafluorophosphate (TBAPF₆) solution to verify the radius of the microdisk.

An 18-cm-long, 1-cm-diameter NMR tube was used as the electrochemical cell. Figure 1 shows the electrochemical cell arrangement and electrode configuration. The NMR tube contained the Pt microdisk (working electrode), a Ag/Ag₂O reference electrode, and a Pt counter electrode. The voltammetric response of the microdisk electrodes was recorded with a Bioanalytical Systems Inc., Model 27-CV, potentiostat and a x-y-t Kipp and Zonen, Model BD90, recorder.

Nitrobenzene, NB (Aldrich, 99+%), was stored over molecular sieves. Acetonitrile (Fisher Scientific, HPLC grade), tetra(*n*-butyl)-ammonium hexafluorophosphate, TBAPF₆ (Sigma), and methanol (Fisher Scientific, HPLC grade) were used as received.

Magnetic Field Characterization. The magnetic field was generated by an open-bore superconducting 400 MHz NMR cryomagnet (Oxford Instruments, Model OX2 ODX). The temperature in the center of the magnet was maintained at $20.1 \pm 0.3 \text{ }^\circ\text{C}$. The *z*-directed component of the magnetic field, B_z , was measured along the centerline *z*-axis of the cryomagnet with an axial Hall probe (F. W. Bell, Model BHA-900). A constant current of 100 mA was passed through the Hall probe through a 50-ohm load and the output voltage was monitored with a Keithley 199 system DMM/scanner. The Hall probe voltage is reported by the manufacturer to be proportional to the magnetic field strength from -30 to $+30$ Tesla (T) with an accuracy of $\pm 2\%$. The Hall probe was calibrated using the value of the magnetic field at the center of magnet ($z = 0$; $B_z = 9.4 \text{ T}$) as an internal standard. This latter value is determined from NMR measurements.

A plot of B_z vs *z*, Figure 2, indicates that B_z decreases from its maximum value at $z = 0$ to negligible values at $z \sim 0.5 \text{ m}$. The gradient of the magnetic field along the *z*-axis, dB_z/dz , is also plotted in Figure

(31) Morris, R. B.; Fischer, K. F.; White, H. S. *J. Phys. Chem.* **1988**, *92*, 5306.

(32) Norton, J. D.; Anderson, S. A.; White, H. S. *J. Phys. Chem.* **1992**, *96*, 3.

(33) Malmsten, R. A.; Smith, C. P.; White, H. S. *J. Electroanal. Chem.* **1986**, *215*, 223.

(34) Paulson, S. C.; Okerlund, N. D.; White, H. S. *Anal. Chem.* **1996**, *68*, 581.

(35) Ragsdale, S. R.; White, H. S. *J. Electroanal. Chem.* **1997**, *432*, 199.

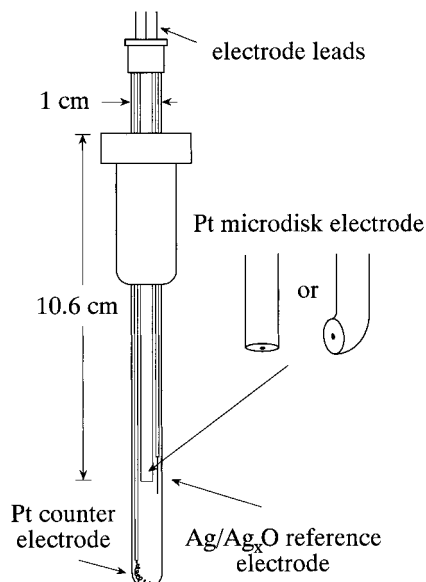


Figure 1. Schematic drawing of the three-electrode electrochemical cell used in this study (approximately to scale). The electrochemical cell is a 1-cm-diameter, 18-cm-long NMR tube, equipped with a Pt auxiliary electrode, a Ag/Ag_xO reference electrode, and the Pt microdisk electrode. The electrochemical cell is lowered into the bore of the superconducting magnet. Two electrode geometries are employed in this study. In the first, the electrode is contained in a straight glass tube, such that the magnetic field is orthogonal to the surface of the microdisk. In the second geometry, the glass tube is bent at a 90° angle, such that the applied magnetic field is directed parallel to the surface of the microdisk.

2. dB_z/dz reaches a maximum of ~ 75 T/m at ~ 0.12 m from the center of the magnet, corresponding to a magnetic field strength of ~ 6 T.

The data in Figure 2 indicate that the magnetic field is nonuniform except at the very center of the magnet. The magnetic field can be described at an arbitrary position, r , using a series expansion around an initial position, $r_0 = 0$,

$$\mathbf{B}(r) = \mathbf{B}_0 + (r \cdot \nabla) \mathbf{B}_0 + \dots \quad (4)$$

where \mathbf{B}_0 is the magnetic field at r_0 . Using a cylindrical coordinate system (r, ϕ, z) to take advantage of the axial symmetry,

$$\mathbf{B}(r) = B_r \hat{r} + B_\phi \hat{\phi} + B_z \hat{k} \quad (5)$$

the components of the magnetic field are as follows:

$$B_r = r \frac{\partial B_r}{\partial r} \quad (6)$$

$$B_\phi = 0 \quad (7)$$

$$B_z = B_0 + z \frac{\partial B_z}{\partial z} \quad (8)$$

Equation 7 indicates that there is no azimuthal component of the field in the cylindrical-shaped cryomagnet.

Because the divergence of the magnetic field is always zero, i.e., $\nabla \cdot \mathbf{B} = 0$, it follows that the decrease in the magnetic field along the z -axis, Figure 2, is accompanied by an increase in the radial component of the field.³⁶ Expanding $\nabla \cdot \mathbf{B} = 0$

$$\frac{1}{r} \frac{\partial}{\partial r} (rB_r) + \frac{1}{r} \frac{\partial}{\partial \phi} B_\phi + \frac{\partial}{\partial z} B_z = 0 \quad (9)$$

and noting that the magnetic field is zero about the azimuth, eq 9

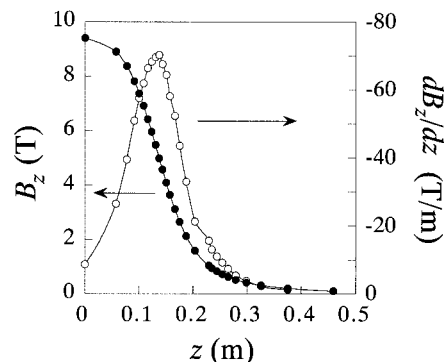


Figure 2. Plot of the magnetic field strength (B_z) and the gradient of the magnetic field (dB_z/dz) versus axial position (z) measured from the center of the magnet ($z = 0$). The largest magnetic field (9.4 T) occurs at $z = 0$. The maximum value of dB_z/dz occurs at $z = 0.12$ m and corresponds to a magnetic field strength of ~ 6.0 T. The solid lines are drawn as a visual guide.

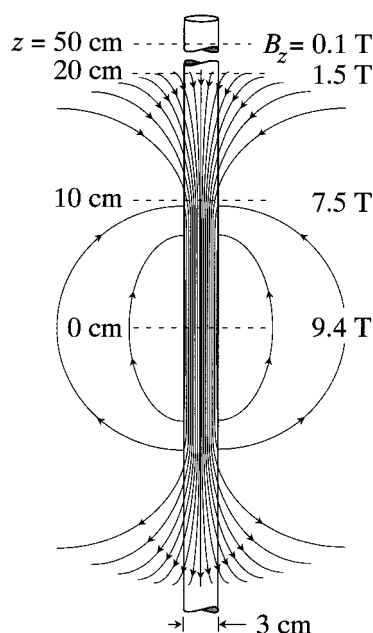


Figure 3. Semicquantitative drawing of the magnetic field lines of the superconducting magnet (3-cm diameter). Values of B_z at several distances (z) from the magnet center are indicated on the drawing.

simplifies to

$$\frac{\partial B_r}{\partial r} + \frac{B_r}{r} = -\frac{\partial B_z}{\partial z} \quad (10)$$

In the limit, $r \rightarrow 0$, the first and second terms in eq 10 are equal; thus,

$$\frac{\partial B_r}{\partial r} = -\frac{1}{2} \frac{\partial B_z}{\partial z} \quad (11)$$

Values of B_r along the z -axis may be calculated from eq 11 by using the measured values of B_z shown in Figure 2. In turn, the values of B_r and B_z allow calculation of the curvature of the magnetic field along the z -axis of the magnet. A semiquantitative representation of the magnetic field is shown in Figure 3. In the electrochemical experiments reported herein, the disk-shaped UME is located directly on the centerline axis and moved between $z = 0$ and 0.5 m with a reproducibility of ± 2 mm.

Results and Discussion

The influence of an external nonuniform magnetic field on electrochemical rates is relatively complex, arising from both

(36) Uman, M. A. *Introduction to Plasma Physics*; McGraw-Hill: New York, 1964; p 52.

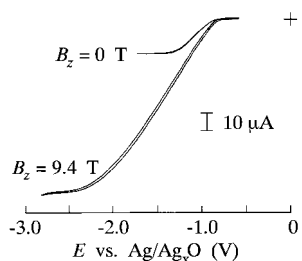


Figure 4. The voltammetric response of a 25 μm -radius Pt microdisk electrode in the absence ($B_z = 0$ T) and presence of a large magnetic field ($B_z \leq 9.4$ T) in an acetonitrile solution containing 1 M nitrobenzene and 0.2 M TBAPF₆. The steady-state current response corresponds to the 1-e⁻ reduction of NB. The magnetic field was oriented *parallel* to the surface of the microdisk. Scan rate = 10 mV/s. The shift in $E_{1/2}$ for the curve recorded in the presence of the magnetic field is due to the decrease in the near-surface solution conductivity.

the MHD force described by Lorentz equation, \mathbf{F}_{MHD} (eq 1), and the gradient force that results from the attraction of the molecular magnetic dipoles into or out of the magnetic field, \mathbf{F}_{VB} (eq 3). Both of these forces are dependent on the magnetic field strength and the field homogeneity. In addition, eq 1 indicates that \mathbf{F}_{MHD} is dependent on the orientation of the magnetic field with respect to the electrode, but independent of the magnetic properties of the redox couple. Conversely, \mathbf{F}_{VB} is dependent upon the *difference* in the magnetic susceptibilities of the two halves of the redox couple, but independent of the field orientation. To acquaint the reader with the electrochemically generated magnetic forces, we first present in Section I a general description of the magnetic phenomena at a disk-shaped UME, accompanied by a qualitative discussion of experimental observations. More quantitative analyses of the magnetic-field effects are explored in Sections II and III, including a numerical evaluation of the two forces, \mathbf{F}_{VB} and \mathbf{F}_{MHD} , acting on the cell during the steady-state electrochemical reaction. Surprisingly, the results indicate that \mathbf{F}_{VB} and \mathbf{F}_{MHD} are of comparable magnitude when a large increase (or decrease) in magnetic susceptibility accompanies the redox chemistry. Depending on the field homogeneity and orientation, \mathbf{F}_{VB} may be much larger than \mathbf{F}_{MHD} , a conclusion that has not been recognized in previous investigations.

I. Voltammetric Behavior of a Disk-Shaped UME in a Nonuniform Magnetic Field. The voltammetric responses of a 25- μm -radius Pt microdisk electrode in the absence ($B = 0$ T, outside the magnet) and presence of a strong uniform magnetic field ($B = 9.4$ T, at the center of the magnet) are shown in Figure 4. The voltammograms were recorded in an acetonitrile solution containing 1 M nitrobenzene, NB, and 0.2 M TBAPF₆ as the supporting electrolyte. The electrode surface in this particular experiment is parallel to the centerline axis of the cryomagnet, corresponding to the electrode with the 90° bend in the glass tubing, Figure 1.

The voltammetric currents correspond to the 1-e⁻ reduction of NB to the radical anion, NB^{•-}, eq 12.



The height of the limiting current plateau reflects the rate at which NB is transported to the electrode surface. Figure 4 shows that the limiting current may be increased by as much as ~400% by a uniform magnetic field.

In discussing the mechanism(s) of the magnetic field effects, it is necessary to briefly recall the basic description of the depletion layer structure at a microdisk electrode. The depletion layer corresponds to the thin layer of solution at the electrode

surface where the electrochemical reaction alters the concentration of the redox reactant, product, and the electrolyte ions. For a disk-shaped UME the thickness of this layer is typically taken as being approximately equal to $5 \times$ the electrode radius. Electroneutrality requires that the negative charge resulting from electrogeneration of NB^{•-} be balanced by an increase and/or decrease in the concentrations of the supporting electrolyte cation (TBA⁺) and anion (PF₆⁻), respectively. This redistribution of electrolyte ions by migrational transport occurs rapidly on the time scale of the slow scan voltammetric experiment. In solutions containing an excess concentration of supporting electrolyte, i.e., $C_{\text{elec}}/C_{\text{redox}} \gg 1$ (where C_{elec} and C_{redox} are the electrolyte and redox concentrations, respectively), the concentration of electrogenerated NB^{•-} is negligibly small in comparison to the concentrations of TBA⁺ and PF₆⁻. In this limiting case, the concentrations of electrolyte ions within the depletion layer are essentially equal to their corresponding bulk solution values. However, excess electrolyte conditions cannot be assumed in the experiments reported here. For example, the voltammetric data shown in Figure 4 correspond to $C_{\text{elec}}/C_{\text{redox}} \sim 0.2$. In this case, the mass-transport limited reduction of 1 M NB requires a significant increase in the concentration of TBA⁺ within the depletion layer to maintain electroneutrality. A concurrent decrease in the depletion layer concentration of PF₆⁻ must also occur. It can be readily shown that $[\text{NB}^{\bullet-}] \approx [\text{TBA}^+]$ and $[\text{PF}_6^-] \approx 0$ are reasonable approximations within the depletion layer when $C_{\text{elec}}/C_{\text{redox}} \ll 1$.

On the basis of the above description of the depletion layer structure, the following scenario is proposed to describe the influence of external magnetic field. Of the four species comprising the solution within the depletion layer (NB, NB^{•-}, CH₃CN, and TBA⁺), only NB and NB^{•-} have nonzero fluxes during the steady-state voltammetric experiments.³⁷ Since NB is electrically neutral, its flux cannot contribute to the magneto-hydrodynamic force, \mathbf{F}_{MHD} . In similar fashion, the gradient force \mathbf{F}_{VB} acting on the paramagnetic product, NB^{•-}, is 2-to-3 orders of magnitude larger, and of opposite direction, than the corresponding force on the diamagnetic reactant, NB, solvent, and electrolyte ions. *Thus, the magnetic force in this experiment is due solely to the interaction of the electrogenerated product, NB^{•-}, with the external field.*

As noted above, the voltammetric currents in Figure 4 reflect the transport-limited electroreduction of the reactant NB; the increase in voltammetric current corresponds to an enhanced flux of NB to the surface. Thus, to explain the magnetic field induced enhancement of current, it is necessary to consider how the magnetic force (either \mathbf{F}_{MHD} or \mathbf{F}_{VB}) exerted on the product, NB^{•-}, results in an enhanced flux of the reactant, NB, to the electrode surface. A mechanism consistent with the experimental observations is that the acceleration of NB^{•-}, by the magnetic field induces convective solution flow, a consequence of the viscous drag of solvent and ions on the electrogenerated ion. The magnetic field-induced fluid convection increases the rate of molecular transfer of NB from the bulk solution to the electrode surface, thus increasing the current at the Pt UME.

Figure 4 also shows that the half-wave potential, $E_{1/2}$, for NB reduction shifts toward negative potentials by ~0.5 V in the presence of the magnetic field. This effect also arises from the magnetic field-induced convection. The flow of solution enhances not only the rate of transport of NB to the surface but also the rate of transport of both the electrogenerated product (NB^{•-}) and counterion (TBA⁺) away from the electrode surface.²² As the external field increases, convective transport

(37) Oldham, K. B. *J. Electroanal. Chem.* **1981**, *122*, 1.

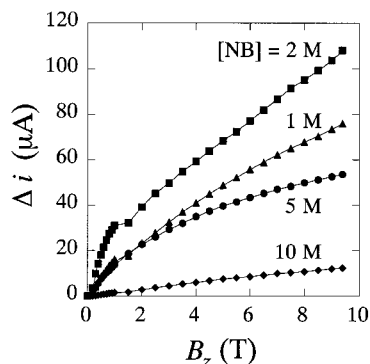


Figure 5. Plot of the change in the voltammetric limiting current (Δi) versus magnetic field strength (B_z). The acetonitrile/0.2 M TBAPF₆ solutions contained 1, 2, 5, or 10 M NB (labeled on the graph). The applied field was oriented parallel to the surface of the electrode. The solid lines are drawn as a visual guide. The change in slope of the curve at ~ 1.5 T for the 2 M solution is an artifact resulting from repositioning the cell inside the magnet during the experiment.

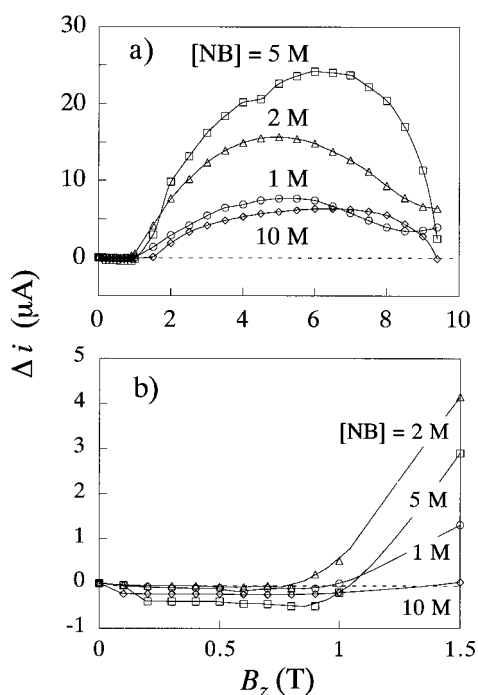


Figure 6. (a) Plot of the change in the voltammetric limiting current (Δi) versus magnetic field strength (B_z). The acetonitrile/0.2 M TBAPF₆ solution contained 1, 2, 5, or 10 M NB (labeled on the graph). The applied field is orthogonal to the surface of the electrode. (b) Enlarged region of the data for $0 < B_z < 1.5$ T. The small negative values of Δi in this regime correspond to cyclotron-like fluid flow. Error bars are approximately the same size as the symbols used to plot the data. The solid lines are drawn as a visual guide.

greatly reduces the concentrations of these ions within the depletion layer, resulting in the depletion layer that has a composition approaching that of the bulk solution. In turn, this decrease in ion concentration causes an increase in the solution resistivity near the surface, resulting in a significant reaction overpotential. The interested reader is referred to a more detailed description of the field-induced shift in $E_{1/2}$ presented in ref 22. The remainder of this paper is concerned only with the magnitude of the limiting current, a quantity not influenced by the ohmic resistive overpotential.

Figures 5 and 6 show the dependence of the current on the magnetic field strength, B_z . Figure 5 corresponds to the electrode with the 90° bend; i.e., the electrode surface is parallel to the

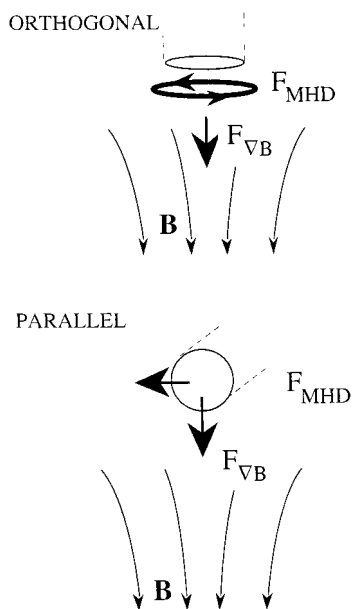
z -axis of the cryomagnet. Figure 6 corresponds to the electrode mounted in the straight glass tubing, such that the electrode surface is orthogonal to the z -axis. Hereafter, we refer to these orientations as “parallel” and “orthogonal”, respectively.

The enhancement in the voltammetric current, Δi , measured relative to the diffusion-limited zero-field value (i.e., $\Delta i = i_{B_z} - i_{B_z=0}$) is plotted as a function of the z -directed component of the magnetic field, B_z . As noted in the Experimental Section, B_z is varied in this experiment by physically moving the electrochemical cell along the centerline axis of the cryomagnet. (A plot of B_z vs z , Figure 2, was previously discussed in the Experimental Section.) It is important to note that it is impossible to vary B_z without varying the gradient of the magnetic field, dB_z/dz . For instance, $B_z = 9.4$ T and $dB_z/dz = 0$ T/m at the center of the magnetic field ($z = 0$); the corresponding values at $z = 0.12$ m are $B_z = 6$ T and $dB_z/dz = 75$ T/m. Because B_z and dB_z/dz vary with z , the magnitudes of the two magnetic forces, \mathbf{F}_{MHD} and \mathbf{F}_{VB} , will also vary with z . Specifically, \mathbf{F}_{MHD} will be largest at the center of the cryomagnet, whereas \mathbf{F}_{VB} is largest at intermediate values of z , approaching zero near the center ($z = 0$) and at the top of the cryomagnet ($z \rightarrow \infty$).

Figure 5 shows that the enhancement in current, Δi , increases steadily with increasing field strength when the electrode is oriented parallel to the magnetic field. The field-induced enhancement in current is largest in solutions containing an intermediate concentration of NB, i.e., the enhancement in current is small in solutions containing either very low or high concentrations of NB. The dependency of Δi on the redox concentration can be understood as follows. In general, the electrochemical current at a UME is expected to be proportional to the reactant concentration.³⁸ However, concentrations of NB greater than ~ 0.1 M result in an increase in viscosity of the acetonitrile solution, which tends to offset the expected increase in current associated with the increase in concentration. Previous studies have demonstrated that NB^{•-} is electrogenerated at a maximum rate in solutions containing ~ 2 M [NB].^{33–35} The magnetic forces, \mathbf{F}_{MHD} and \mathbf{F}_{VB} , are also anticipated to be maximized at this particular solution composition since the flux of charge (\mathbf{J}) in eq 1 and the volume magnetic susceptibility in the depletion layer (χ , relative to the bulk solution value), eq 3, are both proportional to the rate at which NB^{•-} is electrogenerated.

Our previous investigations of magnetic field-induced transport were limited to investigations in uniform fields (i.e., $dB_z/dz = 0$) of strength up to ~ 1 T employing a small benchtop electromagnet.^{21,23} Figure 5 presents data corresponding to magnetic fields that are nearly an order of magnitude larger. The values of Δi for field strengths below 1 T are in good agreement with our previously reported results. This finding is anticipated since the gradient, dB_z/dz , in the cryomagnet is very small when $B_z \leq 1$ T (see Figure 2). Thus, for $B_z < 1$ T, the field is uniform and $\mathbf{F}_{\text{MHD}} \gg \mathbf{F}_{\text{VB}}$. It immediately follows that the enhancement in current at low fields is dominated by the MHD force, eq 1. By using the right-hand rule to evaluate the cross-product in eq 1, it is readily deduced that the net \mathbf{F}_{MHD} acting on the solution adjacent to the electrode is oriented parallel and horizontal to the electrode surface, resulting in the steady flow of solution across the electrode surface. Scheme 1 qualitatively depicts the direction of \mathbf{F}_{MHD} for the parallel electrode orientation.

Figure 6 shows the results of the same experiment, except that the electrode surface is now oriented orthogonal to the magnetic field. In this orientation, a small ($\sim 5\%$) diminishment

Scheme 1. Magnetohydrodynamic (F_{MHD}) and Gradient (F_{VB}) Forces Acting on the Solution Adjacent to the Disk-Shaped UME Surface^a

^a F_{VB} is directed downward, independent of the electrode orientation, corresponding to the movement of electrogenerated paramagnetic species into the magnetic field. F_{MHD} depends on the electrode orientation; it rotates in the plane of the electrode surface when the electrode is oriented *orthogonal* to the field and is directed toward one side of the electrode when the electrode is oriented *parallel* to the field. The rotational force in the *orthogonal* orientation results in cyclotron-like fluid flow, which has a negligible effect on the net flux of redox molecules between the electrode and bulk solution. In this orientation, the observed enhancement in current is due solely to F_{VB} . Both F_{VB} and F_{MHD} contribute to convective transport in the parallel orientation.

of the current is observed at low fields (<1 T), i.e., Δi is negative (Figure 6b). At field strengths greater than ~ 1 T, Δi becomes positive, and increases with field strength until a maximum is reached at $B_z \sim 5.5$ T.

The decrease in current at low fields in the orthogonal orientation agrees very well with previous observations made in uniform magnetic fields generated with use of a benchtop electromagnet.^{21,23} As before, the small decrease in current is clearly due to F_{MHD} (and not F_{VB}) since the field is uniform within the spatial regime of the cryomagnet that corresponds to $B < 1$ T, Figure 2. Previous theoretical analysis of the forces at a disk-shape UME²³ demonstrate that F_{MHD} rotates around the axis of the electrode, as shown in Scheme 1, when the magnetic field is orthogonal to the UME surface. This force creates a cyclotron-like flow pattern in the solution adjacent to the UME surface, as has been recently documented by imaging the spatial distribution of $\text{NB}^{\bullet-}$ with a scanning electrochemical microscope.³⁹ The rotational flow does not bring fresh solution to the electrode surface and, thus, does not enhance the current. However, the rotational flow does effectively eliminate a small component of the flux ($\sim 5\%$) that results from natural convection, the latter being a consequence of the difference in the densities of the depletion layer and bulk solution.²¹ The field-induced decrease in the natural convective flux is solely responsible for the small decrease in current. Ignoring this effect, the rotational flow resulting from F_{MHD} is not expected to have any effect on transport of NB to the electrode surface, regardless of the magnitude of this force. Thus, the increase in current observed at larger fields, $B > 1$ T, cannot be due to F_{MHD} .

(39) Ragsdale, S. R.; White, H. S. Submitted for publication, 1998.

Rather, we propose that this large enhancement is due to F_{VB} , a consequence of the change in magnetic susceptibility that accompanies the electrode reaction.

In the highly concentrated organic solutions, the electrochemical reaction produces a depletion layer that contains molar concentrations of the strongly paramagnetic anion, $\text{NB}^{\bullet-}$. The solution surrounding the depletion layer contains essentially only diamagnetic molecules. The difference in magnetic properties of the depletion layer and bulk solution results in a net force acting on the depletion layer, drawing the electrochemical product toward the center of the cryomagnet where the field is largest. Thus, the force F_{VB} is directed downward away from the electrode surface, as depicted in Scheme 1. As in the case of fluid convection induced by the MHD force, we propose that the concerted motion of electrogenerated paramagnetic molecules results in significant momentum transfer to solvent molecules and electrolyte ions, setting the solution in motion near the electrode surface. Mass balance requires that the downward flow is accompanied by the flow of bulk solution from the edge of the electrode toward the center of the electrode. Interestingly, this flow is in the opposite direction of flow that would be induced by rotation of the electrode, e.g., the classical flow pattern at a rotating disk electrode.

II. Calculation of the Gradient Force.⁴⁰ The gradient force acting on the depletion layer is independent of the orientation of the magnetic field, i.e., F_{VB} does not depend on whether the measurements are made in the parallel or orthogonal orientations, Scheme 1. F_{VB} may be estimated from eq 3, which is simplified to the one-dimensional expression, eq 13, by noting that the radial component of the field, B_r , is zero along the centerline axis.

$$\mathbf{F}_{\text{VB}} = \frac{\chi}{\mu} B_z \frac{dB_z}{dz} \hat{k} \quad (13)$$

Numerical evaluation of F_{VB} requires an estimate of the volume magnetic susceptibility, χ , of the depletion layer in which $\text{NB}^{\bullet-}$ is electrogenerated. A value of χ is obtained from eq 14⁴¹

$$\chi = \Omega \mu_0 \left(\alpha + \frac{\mu_m^2}{3kT} \right) \quad (14)$$

where Ω is the number density of molecules that contribute to χ , α and μ_m are the magnetic polarizability and magnetic dipole moment, respectively, of $\text{NB}^{\bullet-}$, and μ_0 is the permeability of vacuum. The magnetic dipole moment is given by:

$$\mu_m = 2.0023(S(S+1))^{1/2} \mu_B \quad (15)$$

where μ_B is the Bohr magneton (9.274×10^{-24} J/T)⁴² and S is the quantum-spin number. The magnetic spin of the radical anion, $\text{NB}^{\bullet-}$, is assumed to correspond to a single unpaired electron, $S = 1/2$. The paramagnetic contribution to the magnetic susceptibility corresponds to the second term on the right-hand side of eq 14, $\Omega \mu_0 (\mu_m^2 / 3kT)$, and is computed to be equal to 1.60×10^{-8} m³/mol. The diamagnetic contribution, $\Omega \mu_0 \alpha_m$, can be approximated as being equal to the magnetic susceptibility

(40) For the purpose of computing the magnetic forces, we assume that any magnetization that might weaken or enhance the applied field is negligibly small. Thus, we refer to \mathbf{B} as the field and not the magnetic induction.

(41) Atkins, P. *Physical Chemistry*; W. H. Freeman and Co.: New York, 1994.

(42) Cotton, F. A.; Wilkinson, G.; Gaus, P. L. *Basic Inorganic Chemistry*; John Wiley and Sons: New York, 1987; p 64.

of the neutral NB molecule, which is reported as -6.18×10^{-11} m³/mol.⁴³ Thus, the diamagnetic contribution to χ of NB^{•-} is 3 orders of magnitude smaller than the paramagnetic contribution and can be neglected. Similarly, we ignore the contributions to χ arising from the diamagnetic solvent molecules and electrolyte ions.

Combining eqs 13 through 15 and noting that $\mu = \mu_o(1 + \chi) \approx \mu_o$ ⁴⁴ yields the following expression for the magnetic force.

$$\mathbf{F}_{\text{VB}} = \left(\frac{4\Omega\mu_B^2}{3kT} \right) S(S+1) B_z \frac{dB_z}{dz} \hat{k} \quad (16)$$

With the exception of Ω , all parameters in eq 16 are measurable or correspond to physical constants. Ω is estimated as follows: for a mass transport-controlled electrochemical reaction, the concentration of product at the electrode surface (i.e., NB^{•-}) is approximately equal to the concentration of the reactant in the bulk solution (i.e., NB).⁴⁵ Thus, in the most highly concentrated solutions (i.e., 5 M NB), the surface concentration of electrogenerated NB^{•-} is ca. 5 M. This value corresponds to $\Omega \sim 3 \times 10^{27}$ m⁻³.

As an example calculation, we evaluate \mathbf{F}_{VB} for the case where the field gradient is largest (corresponding to $z = 0.12$ m in the magnet). Substitution of $B_z \sim 6$ T, $dB_z/dz \sim 75$ T/m, $S = 1/2$, $\Omega = 3 \times 10^{27}$ m⁻³, and $T = 20$ °C yields $\mathbf{F}_{\text{VB}} = 2.9 \times 10^4$ N/m³.

III. Comparison of \mathbf{F}_{MHD} and \mathbf{F}_{VB} . In this section, we compute values of \mathbf{F}_{MHD} for the parallel and orthogonal orientations, and compare these values with \mathbf{F}_{VB} . Our interest is in the relative magnitudes of these two magnetic forces, for the purpose of determining which force is primarily responsible for the large enhancement in Faradaic currents at the UME. The comparison is made at $z = 0.12$ m, corresponding to the position in the magnet where \mathbf{F}_{VB} has a maximum value equal to 2.9×10^4 N/m³ (see previous section).

In the *parallel* electrode orientation, \mathbf{F}_{MHD} may be calculated by using eq 1, where the flux of charge, \mathbf{J} , at the surface of the electrode is defined by the voltammetric limiting current in the absence of the field, $i_{B_z=0}$, and the electrode radius, a .

$$\mathbf{J} = \frac{i_{B_z=0}}{\pi a^2} \quad (17)$$

In the 5 M NB solution, the limiting current is equal to 23 μ A. Thus, at $z = 0.12$ m, \mathbf{F}_{MHD} is equal to 7.2×10^4 N/m³. Although this value is 3 \times larger than \mathbf{F}_{VB} , we conclude that both forces make significant contributions toward the enhancement of the electrochemical current. It is interesting to note that while \mathbf{J} is proportional to the limiting current, the density of paramagnetic spins, Ω , at the electrode surface will also increase with increasing current. Thus, as a zero-order approximation, the relative magnitudes of \mathbf{F}_{MHD} and \mathbf{F}_{VB} are independent of the solution conditions.

We now consider an analysis of the forces when the magnetic field is *orthogonal* to the disk surface. As previously discussed, in this orientation, the net MHD force is zero and "cyclotron-type" solution flow is generated in the microscopic solution

(43) Weast, R. C. *CRC Handbook of Chemistry and Physics*, 51st ed.; Chemical Rubber Co.: Cleveland, OH, 1971.

(44) Griffiths, D. J. *Introduction to Electrodynamics*; Prentice Hall: Englewood Cliffs, NJ, 1989.

(45) For diffusional transport, mass conservation requires that the concentration of product at the electrode surface be equal to the concentration of reactant in the bulk, if the diffusivities of the product and reactant are equal. This is a reasonable approximation for the redox system reported here.

element near the surface of the electrode. The result of cyclotron fluid motion is a decrease in the limiting current that results from the elimination of natural convection. While this analysis is rigorously correct for a *uniform* field, the nonuniformity of the magnetic field in the experiments described in this article requires a more detailed analysis. The following paragraphs explore this problem.⁴⁶

The current density and magnetic field are related through Ampère's law.⁴¹

$$\nabla \times \mathbf{B}_i = \mu_o \mathbf{J} \quad (18)$$

where \mathbf{B}_i is the internal magnetic field induced by the voltammetric current. \mathbf{B}_i rotates around the center of the electrode, corresponding to the component $B_\phi \hat{\phi}$ in the cylindrical coordinate system. As before, \mathbf{J} corresponds to the current density, or more specifically to the flux of the electrogenerated product, NB^{•-}, away from the electrode surface. By combining eqs 1 and 18, \mathbf{F}_{MHD} is expressed in terms of the total magnetic field, i.e., $\mathbf{B} = \mathbf{B}_e + \mathbf{B}_i$, where \mathbf{B}_e is the external magnetic field.^{41,43}

$$\mathbf{F}_{\text{MHD}} = \frac{1}{\mu_o} (\nabla \times \mathbf{B}) \times \mathbf{B} = \frac{1}{\mu_o} (\nabla \cdot \mathbf{B}) \mathbf{B} - \nabla (B^2/2\mu_o) \quad (19)$$

The first term on the right-hand side of eq 19 describes the magnetic "tension" that results from any curvature of the magnetic field. The second term on the right-hand side of eq 19 describes the magnetic "pressure" exerted on a positive charge toward regions of lower B^2 , or \mathbf{B} . Magnetic pressure and tension result from the inhomogeneity of the magnetic field, and therefore are not observed in uniform magnetic fields. Also, in the absence of moving charges, the magnetic tension and pressure are equal in magnitude, but opposite in direction.

The complexity of eq 19 has prevented the evaluation of \mathbf{F}_{MHD} resulting from the radially divergent flux of ions through a nonuniform field. However, a simpler but related example serves to demonstrate that \mathbf{F}_{MHD} associated with the nonuniformity of the field is negligibly small in comparison to \mathbf{F}_{VB} . Consider a straight wire immersed in the nonuniform field of the cryomagnet employed in this study. The wire is aligned parallel to the centerline of the cryomagnet. Equation 19 then reduces to eq 20,

$$\mathbf{F}_{\text{MHD}} = - \frac{B_\phi}{\mu_o} \left(\frac{B_\phi}{r} \hat{r} + \frac{dB_z}{2dz} \hat{\phi} \right) \quad (20)$$

which indicates that there will be radial (\hat{r}) and rotational components ($\hat{\phi}$) of \mathbf{F}_{MHD} . We assume that the wire has a 25 μ m radius, r_o , and carries a current of 23 μ A (analogous to the actual electrochemical experiments employing the disk-shaped Pt UME). The induced magnetic field is given by Ampère's law as $B_\phi = \mu_o i / 2\pi r_o$. At the surface of the wire, $B_\phi = 1.8 \times 10^{-7}$ T. Substitution of this value into eq 20 yields -1.0×10^{-3} and 5.3 N/m³ for the \hat{r} and $\hat{\phi}$ components of \mathbf{F}_{MHD} at the surface of the wire (these values decrease as one moves further away from the wire). Thus, the component of \mathbf{F}_{MHD} due to the field nonuniformity is vanishingly small. While the preceding analysis is only an approximate treatment of the disk-shaped UME in the orthogonal orientation, we anticipate that \mathbf{F}_{MHD} at the UME will be of the same order of magnitude and, thus, negligibly small in comparison to \mathbf{F}_{VB} .

Having established that \mathbf{F}_{MHD} can be neglected in the orthogonal orientation, it is of interest to examine more carefully the relationship between the enhancement in the electrochemical

(46) Cross, R. C. *Am. J. Phys.* **1989**, *57*, 722.

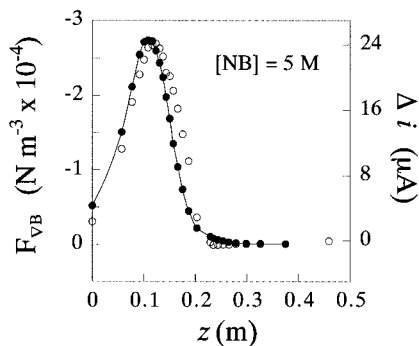


Figure 7. Plot of current enhancement, Δi (open circles), and driving force, F_{VB} (filled circles), versus the position of the electrode in the cryomagnet, z . The solid lines are drawn as a visual guide.

current, Δi , and the driving force, F_{VB} . Figure 7 shows a plot of both quantities versus the spatial position, z , for the 5 M NB solution. It is obvious from this plot that Δi is essentially proportional to F_{VB} , providing the clearest evidence that the enhancement in electrochemical reaction results from acceleration of the electrogenerated paramagnetic ions. To our knowledge, this is the first quantitative demonstration that electrochemical currents can be controlled and enhanced by the interaction of molecular magnetic dipoles with an external magnetic field.

Conclusions

We have demonstrated that two sources of magnetic force are simultaneously operative in an electrochemical experiment,

each capable of significantly increasing the rate of electrochemical reaction. The first of these is the magnetohydrodynamic (MHD) force that arises from the transport of charged reactants and products through the magnetic field. The second force is the gradient magnetic force that arises from electrogeneration of paramagnetic molecules in a nonuniform magnetic field. The latter force is dependent on the magnetic field strength and gradient, and on the magnetic properties of the redox-active molecules. The experiments reported here using the disk-shaped Pt UME's allow the two forces to be separated and individually investigated by variation of the field homogeneity and the electrode orientation. Numerical estimates of the MHD force and gradient forces indicate that these forces are of comparable magnitude in the experiments reported here. Whether or not this conclusion will hold for other redox reactions and electrode geometries remains to be shown.

Preliminary analysis indicates that the enhancement in current resulting from the gradient magnetic force is proportional to the force, i.e., $\Delta i \propto F_{VB}$. This relationship requires further study with molecules having different magnetic susceptibilities and charges. The results suggest that electrochemical currents can be controlled by varying the magnetic susceptibilities of the redox species and the uniformity of the external field.

Acknowledgment. This work was supported by Office of Naval Research.

JA982540Q